SHORT COMMUNICATION

Decoupling of Monsoon Activity across the Northern and Southern Indo-Pacific during the Late Glacial

R.F. Denniston[1]*, Y. Asmerom[2], V.J. Polyak[2], A.D. Wanamaker[3], C.C. Ummenhofer[4], W.F. Humphreys[5,6], J. Cugley[7], D. Woods[8], Stephanie Lucker[1]

[1] Department of Geology, Cornell College, Mount Vernon, IA 52314 USA

[2] Department of Earth and Planetary Sciences, University of New Mexico, Albuquerque, NM 87131 USA

[3] Department of Geological and Atmospheric Sciences, Iowa State University, Ames, IA 50011 USA

[4] Department of Physical Oceanography, Woods Hole Oceanographic Institution, Woods Hole, MA 02543 USA

[5] School of Biological Sciences, University of Western Australia, Crawley, Western Australia, Australia

[6] Western Australian Museum, Welshpool DC, Western Australia

[7] Australian Speleological Federation, Perth, Western Australia, Australia

[8] Department of Parks and Wildlife, Broome, Western Australia, Australia

*Corresponding Author: rdenniston@cornellcollege.edu; Tel: 319-895-4306

key words: stalagmite; carbon isotope; oxygen isotope; Indo-Australian summer monsoon

Abstract

Recent studies of stalagmites from the Southern Hemisphere tropics of Indonesia revealed two shifts in monsoon activity not apparent in records from the Northern Hemisphere sectors of the Austral-Asian monsoon system: an interval of enhanced rainfall at ~19 ka, immediately prior to Heinrich Stadial 1, and a sharp increase in precipitation at ~9 ka. Determining whether these events are site-specific or regional is important for understanding the full range of sensitivities of the Austral-Asian monsoon. We present a discontinuous 40 kyr carbon isotope record of stalagmites from two caves in the Kimberley region of the north-central Australian tropics. Heinrich stadials are represented by pronounced negative carbon isotopic anomalies, indicative of enhanced rainfall associated with a southward shift of the intertropical convergence zone and consistent with hydroclimatic changes observed across Asia and the Indo-Pacific. Between 20-8 ka, however, the Kimberley stalagmites, like the Indonesian record, reveal decoupling of monsoon behavior from Southeast Asia, including the early deglacial wet period (which we term the Late Glacial Pluvial) and the abrupt strengthening of early Holocene monsoon rainfall.

1. Introduction

Integrated within the Austral-Asian monsoon system are the Indonesian-Australian (IASM) and the East Asian summer monsoons (EASM). Hydroclimate reconstructions from Southeast Asia, the Maritime Continent, and northern Australia have revealed that the IASM and EASM responded in a similar, albeit anti-phased, manner during the Younger Dryas (YD) and Heinrich stadials (HS) (Wang et al., 2001; Muller et al., 2012; Ayliffe et al., 2013; Denniston et al., 2013a). During these events, both the austral and boreal summer intertropical convergence zones (ITCZ) drifted southward, producing a weaker EASM and concomitant increases in rainfall over many areas of the Southern Hemisphere within the IASM regime (Reeves et al., 2013). A recent stalagmite record from southern Indonesia (L in Figure 1) identified two pluvial periods lacking counterparts in the EASM: (1) prior to HS1 (Ayliffe et al., 2013) and (2) at the start of the Holocene (Griffiths et al., 2013). Both of these events suggest a southward excursion of the ITCZ unmatched in Southeast Asia. Understanding the spatial scale of these events is useful for evaluating the sensitivities of the IASM and EASM to external forcing. We present a

composite stalagmite record from two caves (B and K in Figure 1) in the monsoon-dominated region of north-central Australia (the southern end of the Austral-Asian monsoon regime) that document the spatial extent of the southward shift of the ITCZ. We focus primarily on stalagmite carbon isotopic ratios, a proxy that reflects a suite of variables specific to the cave sites, but that are linked directly or indirectly to IASM rainfall dynamics. This composite record expands on the previously published oxygen isotopic records of Denniston et al. (2013a; 2013b), with the addition of stalagmites that fill important gaps in the early stages of deglaciation.

2. Cave Locations and Samples

The Kimberley composite stalagmite record involves two cave sites in northern Western Australia separated by ~300 km: Ball Gown cave (17˚2'S, 125˚0'E, ~100 m elevation) and KNI-51 (15˚18'S, 128˚37'E, ~100 m elevation) (Figure 1). Ball Gown cave (western Kimberley) is characterized by anastomosing passageways connecting a single entrance at the top with a single entrance at the bottom of a ~30 m-high escarpment in the Devonian Windjana Limestone. KNI-51 (eastern Kimberley) is formed in the Devonian Ningbing Limestone, and is a shallower cave (~10-15 m) composed of a less complex geometry that is defined largely by a single quasi-horizontal passageway and one entrance (Figure S1; Supplemental Information). We report carbon isotopic ratios of five calcite stalagmites from KNI-51 and six calcite stalagmites from Ball Gown cave. For eight of these 11 stalagmites, age models and oxygen isotopic ratios were previously published (Denniston et al., 2013b); three KNI-51 stalagmite records are newly reported here (Figure S2 and S3). Two of the KNI-51 stalagmites contain evidence for a limited degree alteration of the original finely crystalline fabric, but the facts that (1) both intervals show no evidence of open system behavior with respect to U or Th, and (2) carbon and oxygen isotopic values agree with those in coeval stalagmites, suggest that the climate signals recorded here remain uncompromised. Other short intervals contain evidence of alteration that influenced U-series or stable isotopic ratios, typically just below hiatuses, and data from these areas are excluded from this analysis (Figure S3).

3. Methods

Chronologies for the previously unpublished stalagmite records were developed with 35 ^{230}Th-^{234}U dates obtained at the University of New Mexico using a Thermo Neptune MC-ICP-MS

(Table S1; Supplemental Information). The ages fall in correct stratigraphic order when considering 2σ absolute errors (typically between ±120 to ±380 yr), although some dates were excluded from age models because high $^{232}Th/^{238}U$ ratios led to large corrections for detrital ^{230}Th and thus unacceptably large uncertainties on the ages. Carbon and oxygen ratios were measured at the Iowa State University Department of Geological and Atmospheric Science Stable Isotope Laboratory using a Gas-Bench II with a CombiPal autosampler coupled with a ThermoFinnigan Delta Plus XL continuous flow mass spectrometer (Supplemental Information). Of the total 1,285 samples comprising the Kimberley composite stalagmite time series, 315 were analyzed solely for this study. Environmental conditions (cave air temperature and relative humidity) were recorded as part of an on-going monitoring program at both caves; barometric pressure was also monitored at KNI-51 (Figure S3; Supplemental Information).

4. Results

Oxygen isotopic values in stalagmites are a commonly used proxy for tropical paleohydrology and are related to amount effects in monsoon rainwater, the primary source of oxygen in speleothem carbonate. Analysis of $\delta^{18}O$ values of precipitation from Darwin, Australia, the closest Global Network of Isotopes in Precipitation station to either cave, are closely tied to monthly precipitation amount (IAEA, 2016; Zwart et al., 2016). Carbon isotopic values in stalagmites represent a more complex system, but most drivers of $\delta^{13}C$ variability are tied to hydroclimate over seasonal (Ridley et al., 2015) to orbital time scales (Cruz et al., 2006). Mechanisms linking effective moisture to dripwater (and thus stalagmite) carbon isotopic ratios include prior calcite precipitation (Baker et al., 1997; Ridley et al., 2015), soil biologic activity/vegetation density (Genty et al., 2003), the amount of carbon derived from bedrock (Hellstrom and McCulloch, 2000), and the isotopic composition of overlying vegetation type (influenced by C_3/C_4 ratios and atmospheric pCO_2) (Dorale et al., 1992; Breeker, 2017), all of which are expected to shift $\delta^{13}C$ values higher (lower) during periods of reduced (enhanced) rainfall.

The Kimberley composite stalagmite record yields a continuous time series through the Last Glacial Maximum and deglaciation and spans the majority of the last 40 kyr (Figure 2). Coeval stalagmites from the same cave overlap in isotopic composition and structure, and coeval stalagmites from the two caves also share similar isotopic trends, observations that argue for a

dominant climatic influence on dripwater isotopic chemistry at both sites (Dorale and Liu, 2009). This interpretation is supported by environmental conditions at both caves, and that include high humidity, particularly during the monsoon season when drips are most active and thus when most speleothem growth occurs, and limited seasonal temperature variability (Figure S4). Covariation between $\delta^{13}C$ and $\delta^{18}O$ is low in KNI-51 stalagmites and moderate in Ball Gown stalagmites (Figure S5). Ball Gown and KNI-51 $\delta^{13}C$ values are offset by several permil, with Ball Gown $\delta^{13}C$ values reaching as high as +8‰ while maximum values at KNI-51 are -1‰; Ball Gown stalagmites also exhibit a larger range of values than KNI-51 (15‰ and 10‰, respectively). As a result, stalagmites from each cave are plotted on separate y-axes in order to account for the differential controls on carbon and oxygen isotopic ratios (Figure 2), a method supported (particularly for carbon) by integrating z-scores of these data (Figure S6).

The Kimberley composite stalagmite $\delta^{13}C$ time series largely agrees with the more precisely-dated Liang Luar stalagmite $\delta^{18}O$ records of Griffiths et al. (2013) and Ayliffe et al. (2013) from southern Indonesia (Figure 3). At Liang Luar, as in the Kimberley, HS and the YD are characterized by increases in monsoon rainfall, as recorded by lower oxygen isotopic and/or Sr/Ca ratios. Some discrepancies exist in their respective chronologies, however. While the YD in the Kimberley (13.4-11.7 ka) matches the Indonesian $\delta^{18}O$ record (13.5-11.5 ka), HS1 is dated approximately to 16.5-14.8 ka in the Kimberley and 17.7-14.7 in Indonesia. Average two standard deviation errors on U-Th dates ranging from 24-10 ka are ±230, ±95, and ±150 yr for Hulu Cave, Dongge Cave, and Liang Luar stalagmites, respectively. Similar to the Indonesian stalagmite $\delta^{18}O$ time series, the Kimberley composite stalagmite $\delta^{13}C$ record preserves an interval of enhanced rainfall prior to HS1 (~18.3-17.3 ka in the Kimberley vs ~19.7-19.1 ka in Indonesia). We term this event the Late Glacial Pluvial (LGP). Most of the offsets in age between the Kimberley and Liang Luar time series fall within the combined errors on the ^{230}Th dates, but the LGP is ~1.5 kyr earlier in Indonesia than in the Kimberley. While the structural similarities between the two records suggest the LGP may be the same (or a related) event identified at Liang Luar, the age offset raises questions about their phase relationships and drivers. The offset of the LGP between the Kimberley and Liang Luar records may represent an artifact of dating errors, but it is also possible that the two sites experienced distinct pluvials, or perhaps a single time-transgressive pluvial, in the early stages of deglaciation (Figure 3).

5. Stalagmite Isotopic Variability and Austral-Asian Monsoon Dynamics

While both carbon and oxygen anomalies mark the YD, HS1, and the LGP, the pronounced carbon isotopic anomalies associated with HS2 and HS4 contrast sharply with muted concomitant variations in oxygen isotopic ratios (Figure 2). The reasons for this difference are uncertain but may be related to late glacial sea level variability and the evolution of atmospheric moisture across tropical Australia. In the Kimberley record as at Liang Luar, the magnitude of the LGP is similar to that of HS1; no similar event is apparent in either the Hulu/Sanbao cave records (Wang et al., 2001; Wang et al., 2008) or the Gunung Buda (Borneo) record (Partin et al., 2007).

The second feature apparent in the southern portion of the IASM region is the sharp increase in rainfall at ~9 ka, which is recorded in both KNI-51 and Ball Gown stalagmites (Figure 4). Griffiths et al. (2013) identified this feature in the oxygen isotopic and trace elemental record of Liang Luar stalagmites and tied it to sea level rise and consequent flooding of the Sunda continental shelf, which reached to within 30 m of present sea level by 9.5 ka (Hannebuth et al., 2000) (Figure 4). The synchronous Kimberley carbon isotopic shift also appears linked to enhanced rainfall, likely through a reduction in prior calcite precipitation. However, increases in vegetation density and/or rainforest taxa, such as were observed at ~9 ka in pollen spectra from northern (Shulmeister and Lees, 1995) and northeastern Australia (Donders et al, 2007), could also have played a role. A recent palynological study from the western Kimberley reveals increasing precipitation into the early Holocene but lacks evidence for the abrupt shift to wetter conditions at ~9 ka (Field et al., 2017). Nonetheless, the similarly rapid intensification of the IASM across Indonesia and Australia appears to reveal a regional, rather than local, threshold. Neither this early Holocene monsoon intensification nor the LGP is apparent in either the Borneo (Partin et al., 2007) or Chinese records, however (Wang et al., 2001; Wang et al., 2008) (Figure 4). This finding is consistent with the results of a modeling study by DiNezio and Tierney (2013) which found that exposure of the Sunda Shelf during the Last Glacial Maximum induced regional decreases in rainfall across northern Australia and Indonesia, in part associated with a shift in the location of the Walker Circulation.

6. Conclusions

The Kimberley composite stalagmite $\delta^{13}C$ values appear more sensitive to hydroclimate variability than $\delta^{18}O$ during the Late Glacial and reveals increased rainfall during the YD, HS1, HS2, and HS4, which are matched by concomitant decreases in rainfall in China and/or Borneo, supporting attribution of these events to southward displacement of the ITCZ. However, the presence of pluvials immediately prior to HS1 and at 9.5 ka, events not recorded in the EASM, suggest occasional decoupling of the northern and southern sectors of the Austral-Asian monsoon regime.

Acknowledgements

The authors thank the owners and leaseholders of Carlton Hill Station and the Bunuba People of Windjana. Field assistance provided by Donna Cavlovic, Kym Cugley, Steve Stevets, and James Garrett. Funded by grants from the U.S. National Science Foundation Paleo Perspectives on Climate Change program (AGS-1103413 and AGS-1502917 to RFD) and AGS-1602455 (to CCU and RFD), the Center for Global and Regional Environmental Research, and Cornell College (to RFD). CCU acknowledges support from *The Investment in Science Fund given primarily by WHOI Trustee and Corporation Members*. Support also received from the Kimberley Foundation Australia. We gratefully acknowledge CMAP Precipitation data provided by the NOAA/OAR/ESRL PSD, Boulder, Colorado, USA, from their Web site at http://www.esrl.noaa.gov/psd/. Kimberley stalagmite data are available at the NOAA National Centers for Environmental Information website.

References

1. Ayliffe, L.K., Gagan, M.K., Zhao, J-X., Drysdale, R.N., Hellstrom, J.C., Hantoro, W.S., Griffiths, M.L., Scott-Gagan, H., St Pierre, E., Cowley, J.A., and Suwargadi, B.W. (2013) Rapid interhemispheric climate links via the Australasian monsoon during the last deglaciation. Nature Communications, v. 4, 1-6.
2. Baker, A., Ito, E., Smart, P.L., and McEwan, R.F. (1997) Elevated and variable values of ^{13}C in speleothems in a British cave system. Chemical Geology, v. 136, 263-270.
3. Berger, A. and Loutre, M.F. (1991) Insolation values for the climate of the last 10 million years. Quaternary Science Reviews, v. 10, 297-318.

4. Bintanja, R. and van de Wal, R.S.W. (2008) North American ice-sheet dynamics and the onset of the 100,000-year glacial cycles. Nature, v. 454, 869-872.
5. Breecker, D. O. (2017). Atmospheric pCO2 control on speleothem stable carbon isotope compositions. Earth and Planetary Science Letters, 458, 58-68.
6. Cruz, F.W., Jr., Burns, S.J., Karmann, I., Sharp, W.D., Vuille, M., and Ferrari, J.A. (2006) A stalagmite record of changes in atmospheric circulation and soil processes in the Brazilian subtropics during the Late Pleistocene. Quaternary Science Reviews, v. 25, 2749-2761.
7. Denniston, R.F., Wyrwoll, K-H., Asmerom, Y., Polyak, V.J., Humphreys, W., Cugley, J., Woods, D., Peota, J. and Greaves, E. (2013a) North Atlantic Forcing of Millennial-Scale Australian Monsoon Variability during the Late Glacial. Quaternary Science Reviews, v. 72, 159-168.
8. Denniston, R.F., Wyrwoll, K.-H., Polyak, Brown, J. Asmerom, Y., Wanamaker, A. Jr., LaPointe, Z., Ellerbroek, R., Barthelmes, M., Cleary, D., Cugley, J., Woods, D., Humphreys, W. (2013b) A Stalagmite Record of Holocene Indonesian-Australian Summer Monsoon Variability from the Australian Tropics. Quaternary Science Reviews, v. 78, 155-168.
9. DiNezio, P. N., & Tierney, J. E. (2013). The effect of sea level on glacial Indo-Pacific climate. *Nature Geoscience*, *6*(6), 485-491.
10. Donders, T.H., Haberle, S.G., Hope, G., Wagner, F., Visscher, H. (2007) Pollen evidence for the transition of the Eastern Australian climate system from the post-glacial to the present-day ENSO mode. Quaternary Science Reviews, v. 26, 1621-1637.
11. Dorale, J.A., Gonzalez, L.A., Reagan, M.K., Pickett, D.A., Murrell, M.T., and Baker, R.G., (1992) A high-resolution record of Holocene climate change in speleothem calcite from Cold Water Cave, northeast Iowa: Science, v. 258, 1626-1630.
12. Dorale, J.A. and Liu, Z. (2009) Limitations of Hendy Test criteria in judging the paleoclimatic suitability of speleothems and the need for replication. Journal of Cave and Karst Studies, v. 71, 73-80.
13. Dykoski, C.A., Edwards, R.L., Cheng, H., Yuan, D., Cai, Y., Zhang, M., Lin, Y., Qing, J., An, Z., Revenaugh, J. (2005) A high-resolution, absolute-dated Holocene and deglacial Asian monsoon record from Dongge Cave, China, Earth and Planetary Science Letters, v. 233, 71-86.

14. Field, E., McGowan, H.A., Moss, P.T., Marx, S.K. (2017) A late Quaternary record of monsoon variability in the northwest Kimberley, Australia. Quaternary International, v. 1-17.
15. Genty, D., Blamart, D., Ouahdi, R., Gilmour, M., Baker, A., Jouzel, J., Van-Exter, S. (2003) Precise dating of Dansgaard-Oeschger climate oscillations in western Europe from stalagmite data. Nature, v. 421, 833–837.
16. Griffiths, M.L., Drysdale, R.N., Gagan, M.K., Zhao-J-x., Hellstrom, J.C., Ayliffe, L.K., and Hantoro, W.S. (2013) Abrupt increase in east Indonesian rainfall from flooding of the Suna Shelf ~9500 years ago. Quaternary Science Reviews, v. 74, 273-279.
17. Hanebuth, T., Stattegger, K., and Grootes, P. M. (2000) Rapid flooding of the Sunda Shelf: A late-glacial sea level record. Science, v. 288, 1033–1035.
18. Hellstrom, J.C. and McCulloch, M.T. (2000) Multi-proxy constraints on the climatic significance of trace element records from a New Zealand speleothem. Earth and Planetary Science Letters, v. 179, 287-297.
19. IAEA/WMO: Global Network of Isotopes in Precipitation, The GNIP Database, http://isohis.iaea.org; accessed 2016.
20. Muller, J., McManus, J. F., Oppo, D. W. & Francois, R. (2012) Strengthening of the Northeast Monsoon over the Flores Sea, Indonesia, at the time of Heinrich event 1. Geology, v. 40, 635–638.
21. Partin, J., Cobb, K.M., Adkins, J.F., Clark, B., Fernandez, D. (2007) Millennial-scale trends in west Pacific warm pool hydrology since the Last Glacial Maximum. Nature, v. 449, 452-455.
22. Reeves, Jessica M., et al. (2013) "Palaeoenvironmental change in tropical Australasia over the last 30,000 years–a synthesis by the OZ-INTIMATE group." Quaternary Science Reviews, v. 74, 97-114.
23. Ridley, H.E. et al. (2015) Aerosol forcing of the position of the intertropical convergence zone since AD 1550. Nature Geoscience, v. 8, 195-200.
24. Shulmeister, J. and Lees, B.G. (1995) Pollen evidence from tropical Australia of an ENSO-dominated climate at c. 4000 BP. The Holocene, v. 5, p. 10–18.
25. Wang, Y. J., Cheng, H., Edwards, R. L., An, Z. S., Wu, J. Y., Shen, C. C., and Dorale, J. A. (2001) A high-resolution absolute-dated late Pleistocene monsoon record from Hulu Cave, China. Science, v. 294, 2345–2348, doi:10.1126/science.1064618.

26. Wang, Y., Cheng, H., Edwards, R.L., Kong, X., Shoa, X., Chen, S., Wu, J, Jiang, X., Wang, X., and An, Z. (2008) Millennial- and orbital-scale changes in the East Asian monsoon over the past 224,000 years. Nature, v. 451, 1090-1093.
27. Xie, P. and Arkin, P.A. (1997) Global precipitation: A 17-year monthly analysis based on gauge observations, satellite estimates, and numerical model outputs. Bulletin of the American Meteorological Society, v. 78, 2539 - 2558.
28. Zwart, C., Munksgaard, N.C., Kurita, N., and Bird, M.I. (2016) Stable isotopic signature of Australian monsoon controlled by regional convection. Quaternary Science Reviews, v. 151, 228-235.

Figure Captions

Figure 1. Total mean annual precipitation for Southeast Asia, the Indo-Pacific, and Australia (1979-2015). Stars denote locations of cave sites discussed in text (from north to south): Hulu Cave (H; Wang et al., 2001) and Dongge Cave (D; Dykoski et al., 2005), China; Gunung Buda, Borneo (G; Partin et al., 2007); Liang Luar, Indonesia (L; Griffiths et al., 2013; Ayliffe et al., 2013); KNI-51 (K) and Ball Gown Cave (B), Australia (this study). Dashed oval near K and B denotes location of the Kimberley. Precipitation data from CPC merged precipitation analysis dataset (Xie and Arkin, 1997).

Figure 2. Kimberley composite stalagmite record carbon and oxygen time series. Ball Gown (right axis; earth tones) and KNI-51 (left axis; blues) stalagmite carbon (top) and oxygen (bottom) time series. Note the different scales on the right and left axes, which reflect site-specific controls on speleothem isotopic ratios. Stalagmites from each cave exhibit similar isotopic values and trends, which allows them to be visually integrated into a single time series.

Figure 3. Late Glacial through early Holocene paleomonsoon variability. Oxygen isotopic time series of cave records from **a.** China (Dongge Cave; Dykoski et al,, 2006 – dark blue and Hulu Cave; Wang et al., 2001 – light blue) and **b.** Indonesia (Liang Luar cave; Griffiths et al., 2009 – green; Ayliffe et al., 2013 – blue). **c.** Carbon isotopic time series from Kimberley stalagmites (KNI-51 – blue, left axis; Ball Gown – earth tones; right axis). Dashed lines connect correlated millennial events (YD = Younger Dryas; HS1 = Heinrich Stadial 1; LGP = Late

Glacial Pluvial). For the Kimberley composite stalagmite record, Ball Gown and KNI-51 stalagmites are presented on different y-axes in order to account for the distinct isotopic values and ranges of values at each cave.

Figure 4. Kimberley composite stalagmite isotopic records and regional comparisons. a-f. North-to-south array of stalagmite reconstructions of the Austral-Asian monsoon. **a.** Oxygen isotopic ratios of Dongge cave (Dykoski et al., 2006; dark blue) and Hulu cave stalagmites (Wang et al., 2001; light blue); **b.** Oxygen isotopic ratios from Gunung Buda, Borneo stalagmites (Partin et al., 2007); **c-d.** Oxygen isotopic **(c)** and Sr/Ca ratios **(d)** from Liang Luar, southern Indonesia (Griffiths et al., 2009 - green; Ayliffe et al., 2013 – blue); **e-f.** KNI-51 (black and grey) and Ball Gown (blue and purple) carbon **(e)** and oxygen **(f)** isotopic time series. Isotopic ratios for Ball Gown and KNI-51 are presented on different axes in order to allow the visual integration of the two time series, each of which is influenced by cave-specific controls on both carbon and oxygen; **g.** Eustatic sea level (cyan line; Bintanja and van de Wal, 2008), Indo-Pacific sea surface temperature (purple line; Stott et al., 2002), and June insolation (dashed red line; Berger and Loutre, 1991). Also shown are Heinrich stadials (HS; vertical blue lines), the Younger Dryas (YD), and the Late Glacial Pluvial period (LGP; vertical purple line) identified in the Indonesian and Kimberley records. Gunung Buda record identifies the Antarctic Cold Reversal and not the YD, but neither was demarcated in the figure for ease of interpretation. Red arrows define early Holocene period of enhanced monsoon rainfall. IASM = Indo-Australian summer monsoon; EASM = East Asian summer monsoon.

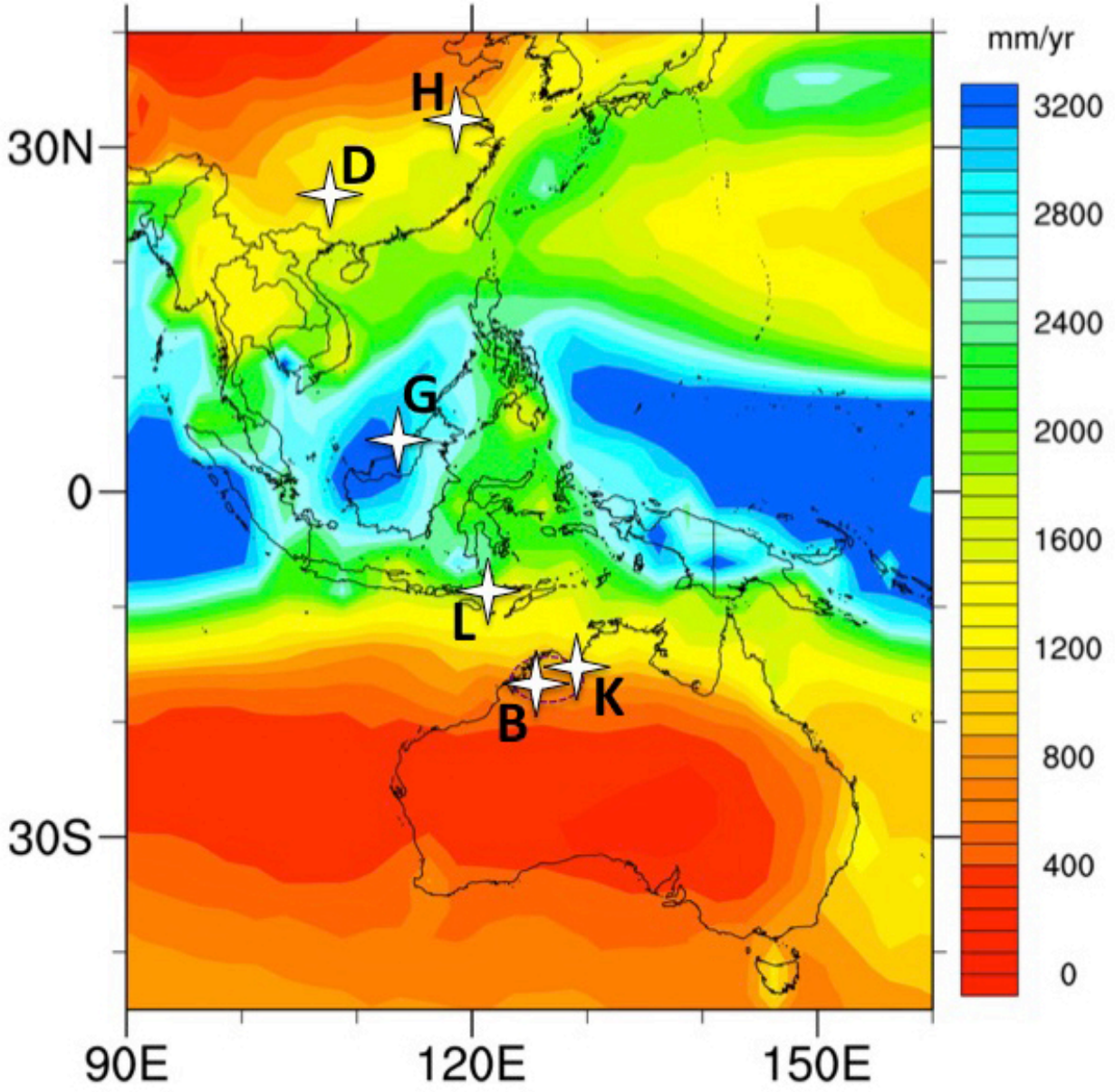
mm/yr
3200
2800
2400
2000
1600
1200
800
400
0
30N
0
30S
90E
120E
150E
H
D
G
L
B
K

Figure 1.

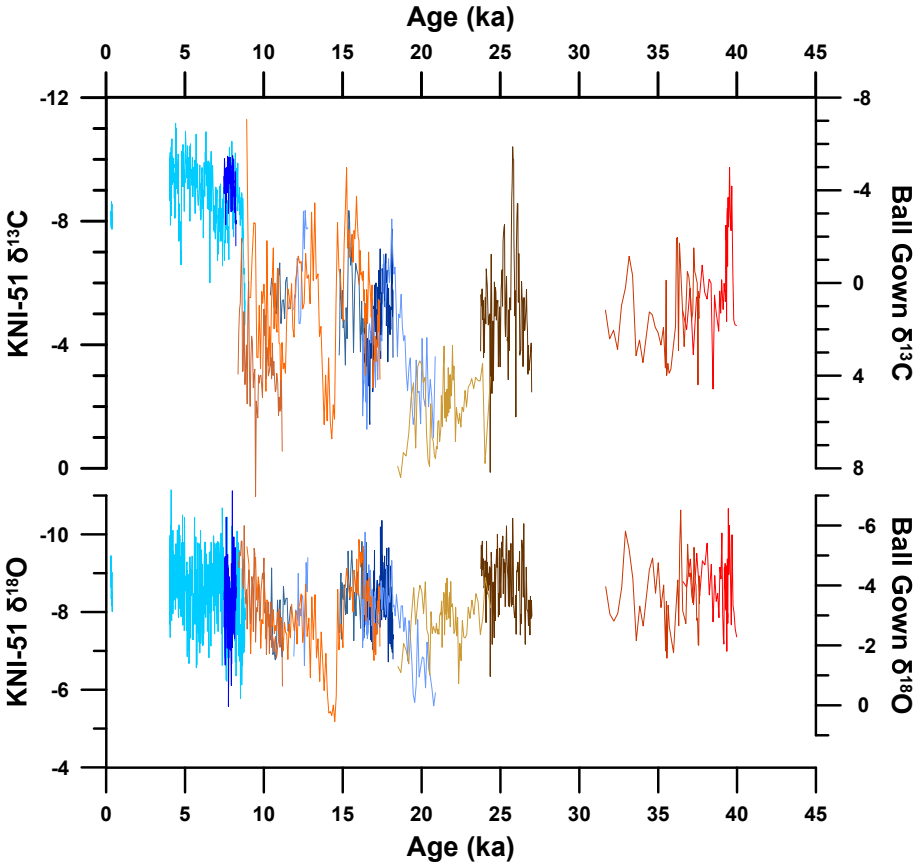
Age (ka)
0
5
10
15
20
25
30
35
40
45
-12
-8
-4
0
KNI-51 δ13C
-8
-4
0
4
8
Ball Gown δ13C
-10
-8
-6
-4
KNI-51 δ18O
-6
-4
-2
0
Ball Gown δ18O
Age (ka)

Figure 2.

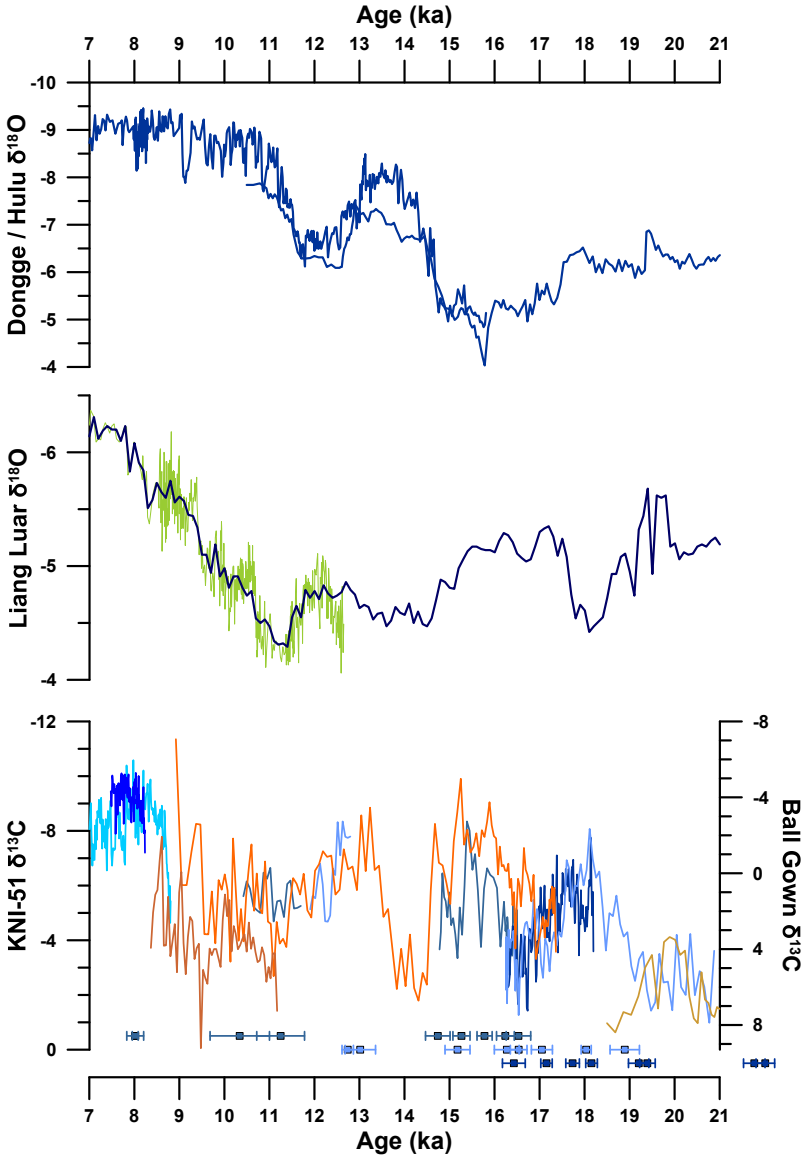
Age (ka)
7 8 9 10 11 12 13 14 15 16 17 18 19 20 21
Dongge / Hulu δ18O
-10 -9 -8 -7 -6 -5 -4
Liang Luar δ18O
-6 -5 -4
KNI-51 δ13C
-12 -8 -4 0
Ball Gown δ13C
-8 -4 0 4 8
Age (ka)
7 8 9 10 11 12 13 14 15 16 17 18 19 20 21

Figure 3

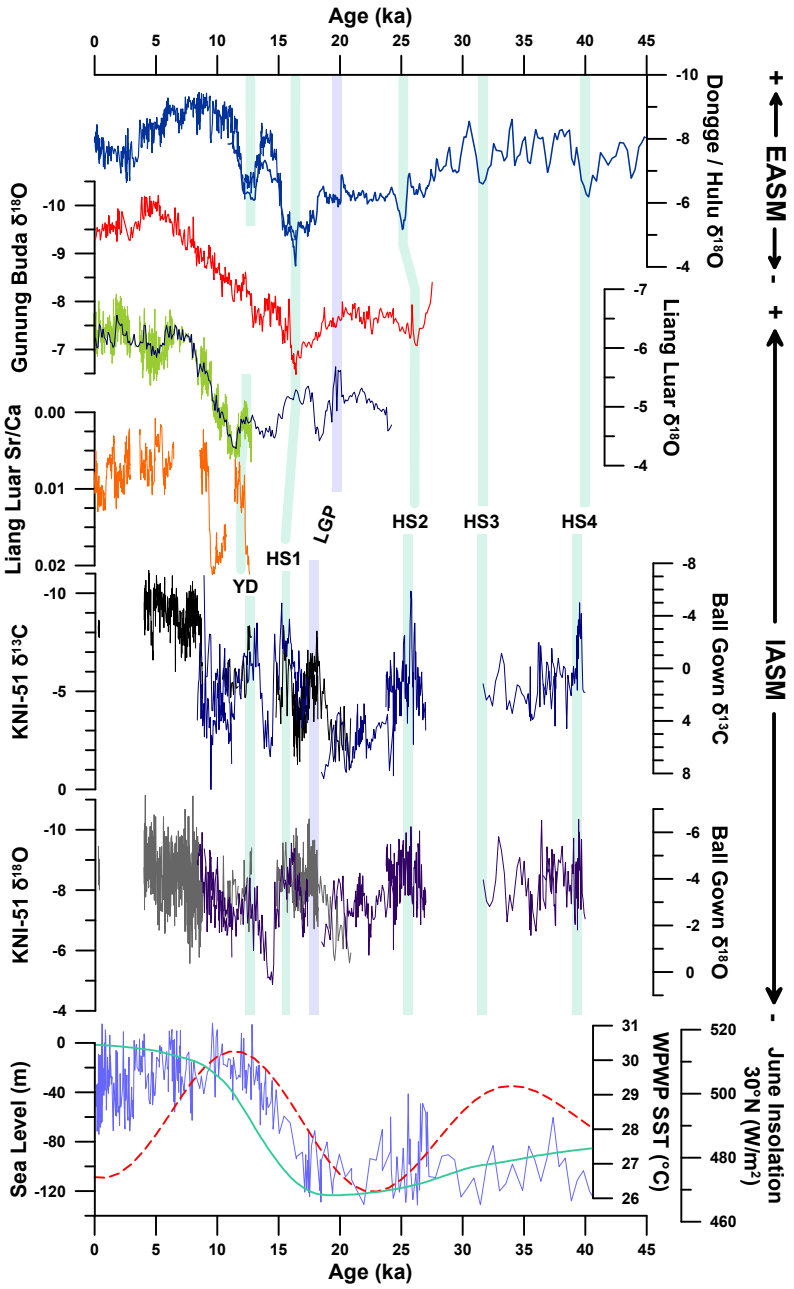
Age (ka)
Dongge / Hulu δ18O
Gunung Buda δ18O
Liang Luar δ18O
Liang Luar Sr/Ca
KNI-51 δ13C
Ball Gown δ13C
KNI-51 δ18O
Ball Gown δ18O
Sea Level (m)
WPWP SST (°C)
June Insolation 30°N (W/m2)
EASM
IASM
LGP
HS1
HS2
HS3
HS4
YD

Figure 4